ISOTOPES IN ENVIRONMENTAL AND HEALTH STUDIES, 2017
VOL. 53, NO. 5, 500–517
https://doi.org/10.1080/10256016.2017.1355795

Hydrology of the North Klondike River: carbon export, water balance and inter-annual climate influences within a sub-alpine permafrost catchment

Anthony Lapp[a], Ian D. Clark[a], Andrew L. Macumber[b] and R. Timothy Patterson[b]

[a]André E. Lalonde Accelerator Mass Spectrometry (AMS) Laboratory, University of Ottawa, Ottawa, Ontario, Canada; [b]Faculty of Science, Carleton University, Ottawa, Ontario, Canada

Dedicated to Professor Peter Fritz on the occasion of his 80th birthday

ABSTRACT
Arctic and sub-arctic watersheds are undergoing significant changes due to recent climate warming and degrading permafrost, engendering enhanced monitoring of arctic rivers. Smaller catchments provide understanding of discharge, solute flux and groundwater recharge at the process level that contributes to an understanding of how larger arctic watersheds are responding to climate change. The North Klondike River, located in west central Yukon, is a sub-alpine permafrost catchment, which maintains an active hydrological monitoring station with a record of >40 years. In addition to being able to monitor intra-annual variability, this data set allows for more complex analysis of streamflow records. Streamflow data, geochemistry and stable isotope data for 2014 show a groundwater-dominated system, predominantly recharged during periods of snowmelt. Radiocarbon is shown to be a valuable tracer of soil zone recharge processes and carbon sources. Winter groundwater baseflow contributes 20 % of total annual discharge, and accounts for up to 50 % of total river discharge during the spring and summer months. Although total stream discharge remains unchanged, mean annual groundwater baseflow has increased over the 40-year monitoring period. Wavelet analysis reveals a catchment that responds to El Niño and longer solar cycles, as well as climatic shifts such as the Pacific Decadal Oscillation.

ARTICLE HISTORY
Received 11 January 2017
Accepted 11 July 2017

KEYWORDS
Carbon-13; carbon-14; catchment; groundwater; hydrogen-2; hydrogen-3; isotope hydrology; North Klondike River; oxygen-18; sub-alpine permafrost; water balance

1. Introduction

The hydrology of arctic and sub-arctic watersheds is changing due to recent climate warming [1–3]. Permafrost temperatures have warmed across the northern hemisphere in recent decades [4,5], which has profound implications for storage, recharge processes and subsequent effects on seasonal discharge. Changes in ecosystems have already been observed in sub-arctic regions as water budgets begin to change [6]. Groundwater behaviour in permafrost environments is an understudied topic, and has seen relatively

CONTACT Anthony Lapp alapp@uottawa.ca

This article has been corrected with minor changes. These changes do not impact the academic content of the article.
This article was originally published with errors. This version has been corrected. Please see Corrigendum (https://doi.org/10.1080/10256016.2017.1371423).

little research over the past decade [7–10]. Although recent concerns about climate change have generated an increased interest in high-latitude hydrology research, the widespread operational decline in river discharge monitoring in both North America and Eurasia will hinder future work [11].

The majority of reporting on discharge response to climate has been observed on large river systems in Canada and the United States such as the Yukon and Porcupine Rivers [2], the Mackenzie and Peel River [12] and on large Russian rivers [13–15], with little attention to flow processes in headwater catchments. Thawing permafrost has been hypothesized to allow deeper groundwater contribution to the drainage network and an increased active layer thickness resulting in deeper supra-permafrost pathways [16–18] and a change in the seasonality of discharge. Although total annual discharge has remained fairly constant in most northern watersheds, an increase in average winter and spring flows has been observed [19]. However, the analysis and understanding of inter-annual and inter-decadal hydrological variability has often been limited to southern watersheds [20,21], and to short periods in northern watersheds [22]. The analysis of time series can provide an important perspective on the nature of hydrological variability with changing climate.

There have been several studies assessing carbon export within arctic watersheds and its potential to serve as indicators of permafrost thaw, with a focus on large river systems [2,23,24], and less on small-scale catchments [2,16,17,25,26]. Raymond et al. and other studies [27–29] monitored dissolved organic carbon (DOC) quantity and age in the largest arctic rivers (Yenisey, Lena, Ob', Mackenzie, Yukon), showing that these arctic rivers export ~2.5x more organic carbon than similar temperate rivers and establishing baseline data for assessment of changes with climate. However, the ability to observe and quantify changes in DOC within the watershed is made more complicated by the size and diversity of sub-watersheds within the Yukon River basin. A more effective strategy to assess climate-based influences in arctic river basins would include the identification and monitoring of smaller tributaries sensitive to glacial melting, permafrost thaw and changes in watershed hydrology in addition to large headwater catchments. The hydrological transition to less permafrost has been hypothesized to show a decline in DOC by rerouting subsurface flow through deeper mineral soils previously isolated by permafrost [12,17,30]. Understanding meltwater pathways is then essential for understanding carbon export within catchments.

The North Klondike River (NKR), with its long-term hydrological monitoring record, was selected to study groundwater recharge processes in a small-scale permafrost catchment. Located in the Yukon's Tombstone Territorial Park, this river is ideal for the study of groundwater hydrology in a discontinuous permafrost zone, as the NKR valley lies right on the boundary between discontinuous and continuous permafrost. The Yukon government has maintained a hydrologic monitoring station for a period of approximately 40 years (1974 to present). This long-term streamflow record is useful for measuring any changes or long-term trends in stream flow and baseflow behaviour.

This study seeks to combine an understanding of weathering, carbon and groundwater recharge processes with an assessment of intra-annual discharge variability within a sub-alpine permafrost catchment. Hydrograph separation techniques are linked with dissolved ion hydrochemistry, dissolved carbon and hydrometric conditions to determine stream flow behaviour and seasonal groundwater contribution to total stream discharge.

Statistical methods are then used to analyse the long-term record for inter-annual and inter-decadal hydrological changes or patterns.

2. Geology, physiography and hydrology of the North Klondike watershed

The NKR (N 64°00′07.1″, W 138°35′45.0″) is a 1100 km^2 headwater catchment situated in the West Central Yukon, approximately 68 km northeast of Dawson City. The NKR has its source in the southern Ogilvie Mountains, within Tombstone Territorial Park, and is a tributary of the Klondike River in the Yukon River watershed. Approximate latitudes of the NKR valley range from 64°00′ to 64°30′N and approximate longitudes from 138°00′ to 138°45′W, with an elevation range from 600 to 1000 m above sea level. Figure 1 shows the NKR watershed including the meteorological station, as well as the discharge monitoring station where samples were taken.

The NKR resides in the Mackenzie Mountain ecoregion and separates the northern Yukon from the central Yukon. The entire ecoregion lies within the Cordilleran Foreland Fold and Thrust Belt, with the rock units and structures largely defining the landscape. Valley bottoms and the lower portion of the catchment are unconsolidated glacial and alluvial deposits, left behind from localized valley glaciation, and dominate valley bottoms and the lower portion of the catchment. The geology of the basin is primarily crystalline rock units, with areas of igneous intrusions and extensive faulting within the Tombstone Mountain range.

The NKR contains an area of aufeis, a sheet-like mass of layered ice formed by the successive flows of groundwater discharge from the river bed [31]. This aufeis, located upstream of the Tombstone Park Interpretive Center, is an excellent indicator of a strong groundwater presence within the watershed. The NKR has a mean annual discharge of 3.92×10^8 m^3, mean annual temperature of −4 °C, and mean annual precipitation of 309 mm.

Kojima [32] provided a study of vegetation within the valley. The NKR valley belongs to the boreal forest region, characterized by coniferous forests interspersed with wetlands and bogs. Soils are rich in organic material with high carbon storage, and are underlain with permafrost at a depth of approximately 30–40 cm. Gentle lower slopes of the valley are entirely covered by closed forests consisting of white spruce and the occasional black spruce. Above the forest line, 1000 m above sea level on south slopes and 800 m on north slopes, close forest changes to open woodland, followed by extensive shrub tundra and dwarf birch [32].

Although this ecoregion straddles the southern boundary of the continuous permafrost zone, permafrost is found almost entirely throughout this region due to the elevation, with near surface temperatures above −4 °C. Permafrost is very extensive within the valley and on north-facing slopes where peat can accumulate and provide insulation [32,33].

3. Methods

3.1. Sample and data collection

Field work was conducted between August 2013 and August 2014. Preliminary sampling was conducted on 1–25 August 2013, to determine sampling logistical requirements as well as contacting and enlisting local personnel for sample collection. Water samples were taken

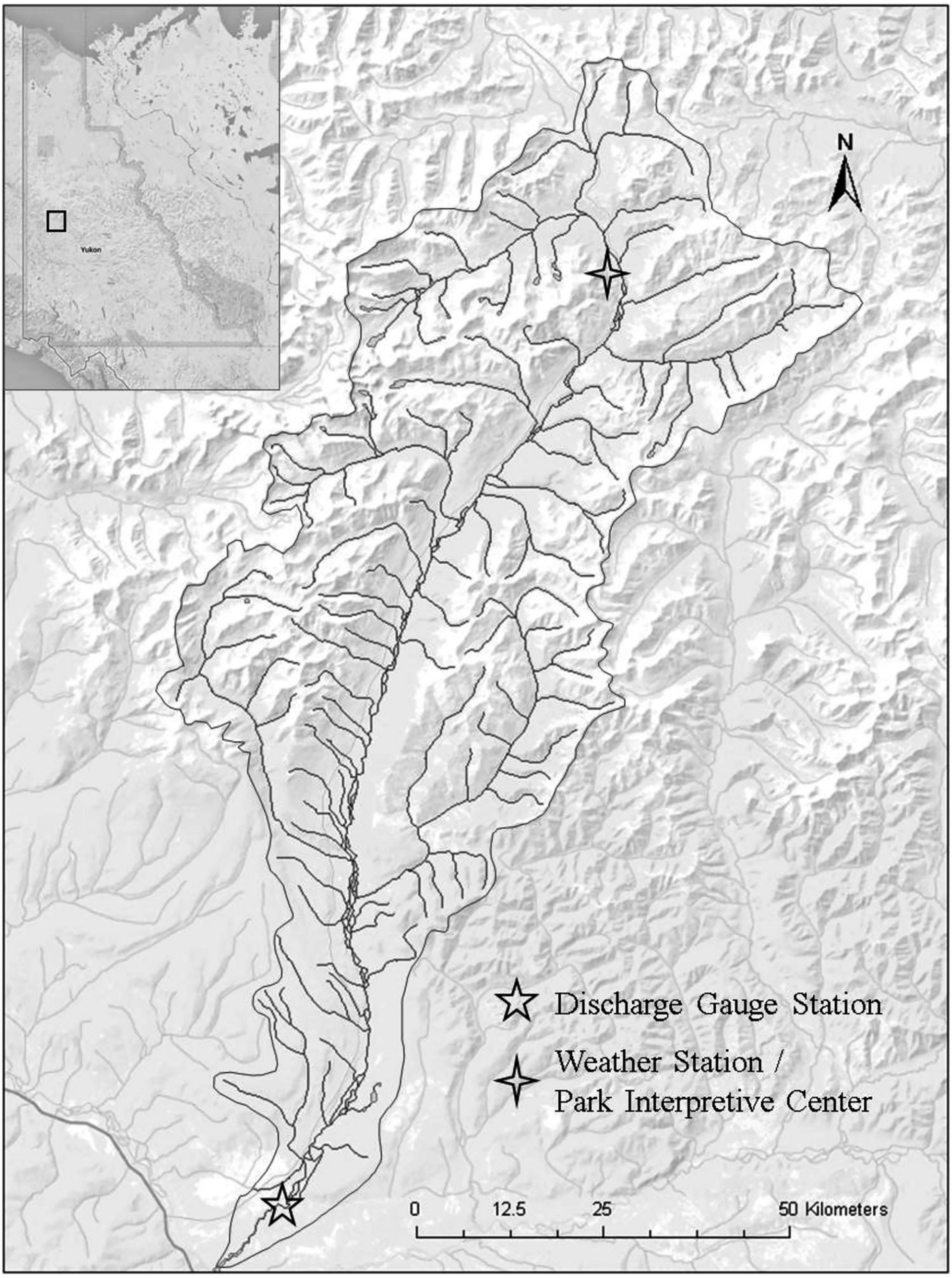

Figure 1. The NKR valley, Yukon, Canada. The weather station, park interpretive centre and the discharge gauge station are marked on the map. Samples were taken near to the gauge station. The location of the NKR within the Yukon territory is shown in the top left.

from the NKR by the Yukon Government Highway Tombstone maintenance camp from 7 January to 19 August 2014, approximately every 2 weeks from near to the gauge station. River water was taken in clean, sterile, 1-L Nalgene bottles. All samples were shipped back to the Advanced Research Complex at the University of Ottawa for analyses. Water samples were filtered using 0.45 µm nitrile filters and aliquoted into 10-ml falcon tubes for geochemical analysis, and 40 ml EPA vials for DOC, dissolved inorganic carbon (DIC) and $\delta^{13}C$ analysis. Water required for radiocarbon was filtered using 0.45-µm nitrile filters and injected into a clean, sterile, baked, and evacuated 1-L glass bottle prior to CO_2 extraction.

Precipitation was collected at the Dawson City Airport from 1 August 2013 to 23 August 2014, in order to establish a Local Meteoric Water Line (LMWL). The difference in elevation between Dawson City and the NKR catchment is less than 500 m and would impart only a minor shift in isotope values of less than 2 ‰. Spring sampling of the NKR was undertaken from 14 April to 8 May 2014 to sample pre-freshet discharge under ice and during spring freshet. Climate data were provided by the Government of Canada and Environment Yukon. Yukon Parks provided climate data for 2014 from within the NKR basin at the Tombstone Interpretative Center.

3.2. Laboratory analysis

Major ion concentrations were measured in the Geochemistry Lab at the University of Ottawa. Field-filtered samples for cation analysis were acidified in the lab with nitric acid and measured by inductively coupled plasma emission spectroscopy (Vista-ICP-OES), and anions were measured by an ion chromatograph (Dionex ICS-2100). $\delta^{18}O$ and $\delta^{2}H$ were analysed by laser absorption spectroscopy using a Los Gatos Research liquid water isotopic analyzer (Model LWIA-24d). Measurement precision for $\delta^{2}H$ is ±1 ‰ and ±0.25 ‰ for $\delta^{18}O$, with respect to Vienna Standard Mean Ocean Water (VSMOW). Total and dissolved inorganic/organic carbon were first measured by OI Analytical Aurora Model 1030W TIC-TOC analyzer to measure ppm of C, followed by analysis for $\delta^{13}C$ [34]. The TIC-TOC is interfaced to a Finnigan Mat DeltaPlusXP isotope ratio mass spectrometer for analysis by continuous flow. Data are normalized using three different internal organic standards, with an analytical precision of 2 % for carbon concentrations (ppm) and ±0.2 ‰ for $\delta^{13}C$. Tritium (^{3}H) activity in water was analysed by liquid scintillation counting on a Quantalus 1220 low level liquid scintillation counter. Due to the low tritium content of the water, the samples had to be enriched using an electrolytic enrichment method at the University of Ottawa Radiohalide Lab. Counting results were reported in Bq/L and in tritium units (TU), with a limit of detection of 1.1 Bq/L. Water from mid-Holocene glacier ice was used as a blank for background correction. The standard used in the calibration for Quantalus 1220 is certified standard SRM 4926E activity 0.0028 mCi ^{3}H water from National Institute of Standards and Technology. Dissolved inorganic and organic carbon was extracted from water as CO_2, then graphitized for ^{14}C analysis on the accelerator mass spectrometer (AMS) in the A.E. Lalonde AMS Laboratory at the University of Ottawa Advanced Researched Complex. Iron powder was used as a catalyst to reduce the conversion time of CO_2 to graphite, which takes place under hydrogen environment. Standards of oxalic acid were provided by the University of Ottawa Radiocarbon Lab, and individual analyses are accompanied by their analytical uncertainty.

3.3. Data analysis

Stream hydrograph separation was undertaken to establish the seasonal variation for groundwater contributing to the basin using established isotope and geochemical approaches [22,35–38]. This groundwater discharge is essentially the only source of river water in the winter [39]. A three-component mixing model was used to distinguish groundwater from surface runoff, according to:

$$Q_t = Q_{gw} + Q_{alw} + Q_p, \tag{1}$$

where Q_t is the total stream flow, Q_{gw} the contribution from sub-permafrost groundwater, Q_{alw} the contribution from soil water in the active layer and Q_p the contribution from direct precipitation and runoff. Solution of a three-component mixing model requires two tracer solutes and uses simple mass balance equations [38]. For the NKR, SO_4^{2-} was used as geogenic tracer, and both K^+ and DOC were used as pedogenic tracers. Endmember concentrations for groundwater were taken from the river concentrations in early April before the spring freshet. For active layer water, values at 120 % of the freshet were used, although the final separations were found to be relatively insensitive to this value. Values for precipitation were taken to be negligible.

Statistical treatment of historical discharge data were undertaken using spectral techniques for these time series data. Environment Canada provides the daily mean discharge data for the NKR from 1975 to 2014. The non-parametric Mann–Kendall test was used to test for temporal trends in maximum and minimum discharge and their timing, baseflow (defined as flow from January to April), snow pack thickness, precipitation and total annual flow using the Mann–Kendall test for trend. The analysis was performed using XL Stat, a statistical software plugin for Microsoft Excel. Spectral analysis was performed on mean monthly river discharge, baseflow and nine hydrologic variables for the NKR to identify significant cycles related to climate phenomena. The North Klondike discharge data set consists of 480 observations, each a monthly mean, spanning from 1977 to 2014. The software PAST (v3.12) was used for time series analysis [40–42].

4. Results and discussion

4.1. Fluvial regime of the NKR

Figure 2 shows discharge, maximum and minimum temperatures and precipitation recorded in Tombstone Territorial Park for 2014. Snowmelt is the dominant hydrometric event in sub-arctic catchments. As such, most streams are characterized by their response to different melting regimes. Furthermore, this catchment has no significant surface water bodies, and is unaltered by human activity, apart from a few cabins and one culvert section to accommodate the crossing of the Dempster highway. The NKR would be considered a sub-arctic nival (snow-dominated) and spring-fed regime [43]. Characteristics of these regimes include:

(1) snowmelt as a prominent feature of discharge,
(2) long stream flow seasons,
(3) frequent increases in summer flow produced by rainfall events,
(4) low flow period during the winter, maintained by groundwater discharge through taliks in discontinuous permafrost creating a relatively stable stream flow.

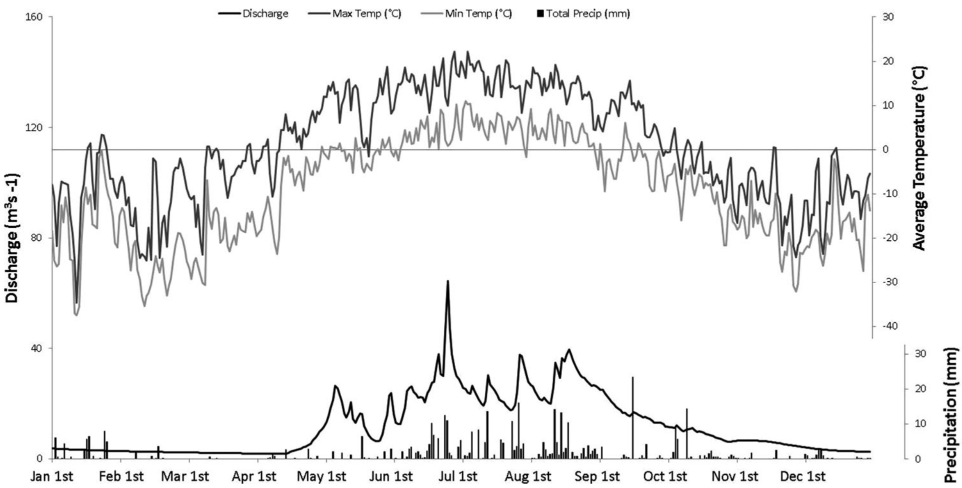

Figure 2. NKR hydrograph, with precipitation and minimum and maximum temperatures plotted for 2014.

For 2014, the average total river discharge during winter months preceding river break and spring freshet is 3.1 $m^3 s^{-1}$, higher than average historical baseflow discharge of 2.7 $m^3 s^{-1}$. The NKR broke on approximately 28 April 2014, followed by the beginning of spring freshet and the contribution of snowmelt. Peak discharge is not seen until June, when minimum temperatures remain above 0 °, coupled with summer rain events. Sub-arctic regions have a high percentage of precipitation arriving as snow on the ground, lasting from October/November to March/April [39]. Spring freshet for 2014 showed a less-typical, muted discharge peak during a prolonged snowmelt period due to a cooler spring and a thinner than usual snow pack. Compared with temperate latitudes, the arrival of snowmelt in sub-arctic regions or high mountains can be delayed by weeks or even months. Following peak discharge, total river discharge begins to decrease towards average baseflow discharge unless supplemented by summer and fall rain storm events. Total annual runoff represents 80 % of total annual precipitation for the region. This high coefficient of runoff is typical for permafrost landscapes where the frozen active layer precludes infiltration for much of the melt season.

4.2. NKR historical hydrometric data: Mann–Kendall and wavelet analysis

Monitoring of the fluvial regime over the past 40 years shows considerable year-to-year variability in the magnitude and timing of seasonal discharge. Mann–Kendall and wavelet analysis of these time series demonstrate this variability to be in part driven by solar cycles. The results from the non-parametric Mann–Kendall trend test show no statistically significant trends in precipitation, maximum and minimum discharge and their timing, snow pack thickness, precipitation, and total annual flow, at the 95 % confidence interval. However, for mean annual baseflow ($p = .002$, characterized by mean flow from January to April). Kendall's tau of 0.389 suggests an increase from 1975 to 2014. This increase in baseflow has not significantly affected total annual discharge, which exhibits no measured trend.

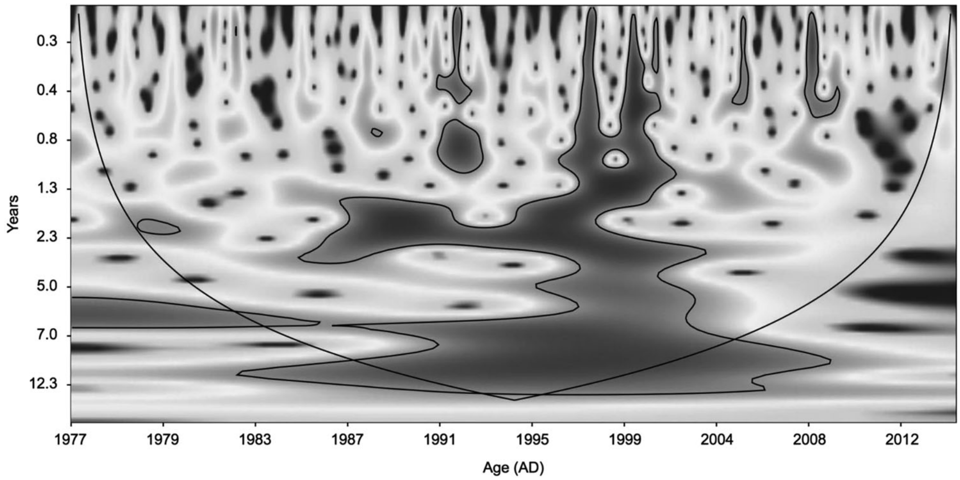

Figure 3. Results of the Morlet wavelet transformation, with power exceeding significance ($p < .05$) outlined on the diagram. The *y*-axis represents the frequency in years ($1/x$) and the *x*-axis represents time (AD).

Figure 3 shows the results of the Morlet Wavelet transformation for the North Klondike mean monthly discharge values. Figure 4 shows the significant periodicities within the data set at the 95 % confidence interval.

The spectral and wavelet analysis results of the NKR show a sub-alpine catchment sensitive to global climatic and solar changes. The short 2.7-, 3.5- and 5.6-year periods are thought to be El Niño–Southern Oscillation events. The 11-year Schwabe solar sunspot cycle is also present in the data set, represented by the 10.9 periodicity. Imprinted over these cycles are the Pacific Decadal Oscillation (PDO) regimen shifts in the North-East

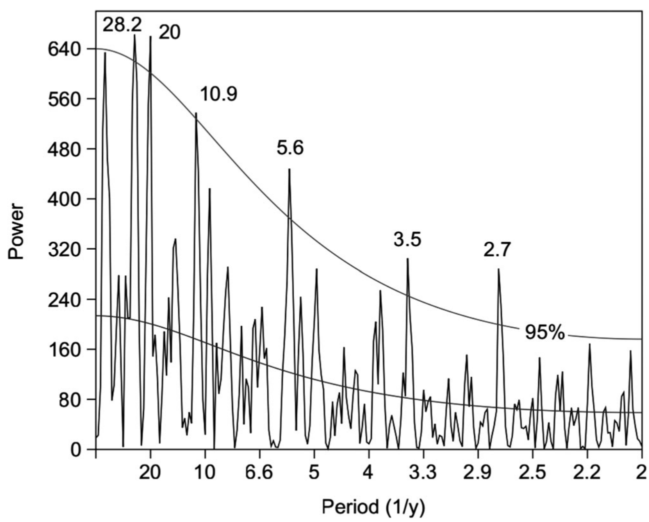

Figure 4. Significant periodicities within the NKR monthly mean data set, with the 95 % significance level line plotted.

Pacific. This demonstrates a significant solar and climatic influence on the NKR basin. Further work is being carried out to determine the effects of these cycles on basin hydrology, and their potential effects on groundwater contribution to discharge.

4.3. Recharge origin and age – $\delta^{18}O$, $\delta^{2}H$ and ^{3}H

Precipitation collected at the Dawson City airport during 2013 and 2014 was used to establish a local meteoric water line for the area (Figure 5). Samples were collected after precipitation events within that time period. The equation for the LMWL in Dawson is $\delta^{2}H = 6.3\ \delta^{18}O - 35.7$, a slope slightly lower than the GMWL, with a slope of ~8.

$\delta^{18}O$ and $\delta^{2}H$ values in the NKR show distinct seasonal trends. During the winter months (October–April), values plot close to the LMWL, which is consistent with a groundwater-dominated system recharged by precipitation, specifically snowmelt. As the river breaks and with the arrival of spring freshet, isotopic values shift above the LMWL and become slightly depleted.

Precipitation from 2013 to 2014 plots over a range of close to −20 ‰ for $\delta^{18}O$, while the range for NKR is less than 1 ‰, indicating considerable attenuation of seasonal variability due to mixing and storage within the watershed (Figures 6 and 7). The temporal trend for $\delta^{18}O$ in the NKR shows a depletion of 0.5 ‰ in May, which coincides with spring freshet due to the contribution of snowmelt with lower $\delta^{18}O$ values. $\delta^{18}O$ shows another depletion event in July, coinciding with maximum river discharge. This isotopic response has been observed in other permafrost catchments [22], due to mixing of groundwater/soil water with snowmelt water. Further, NKR values are close to the median value for winter precipitation which must therefore contribute significantly to recharge.

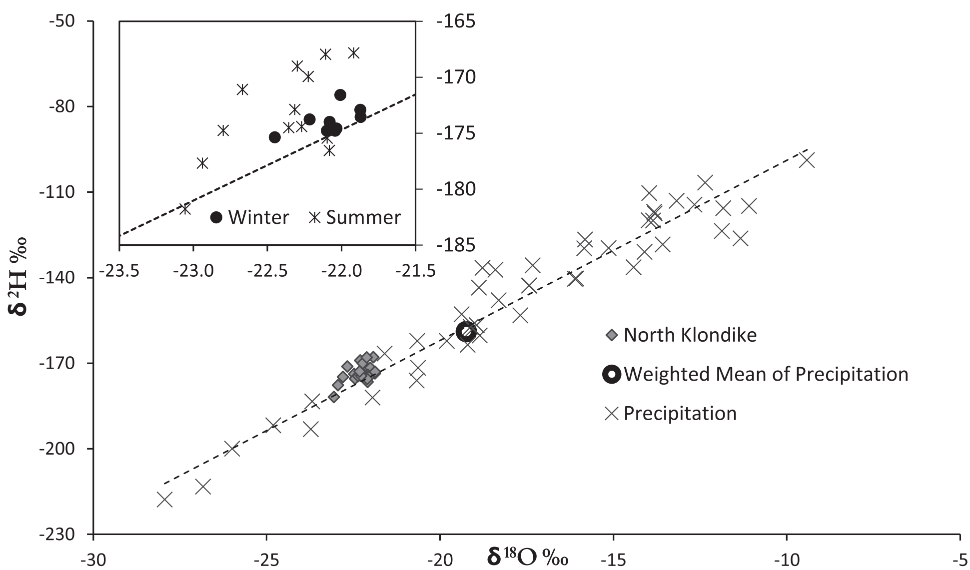

Figure 5. Deuterium and oxygen-18 (VSMOW) of rainwater collected at Dawson City Airport (2013–2014) and NKR water (2014). The dotted black line represents the LMWL at Dawson Airport. The insert shows the seasonal breakdown of the NKR water for 2014.

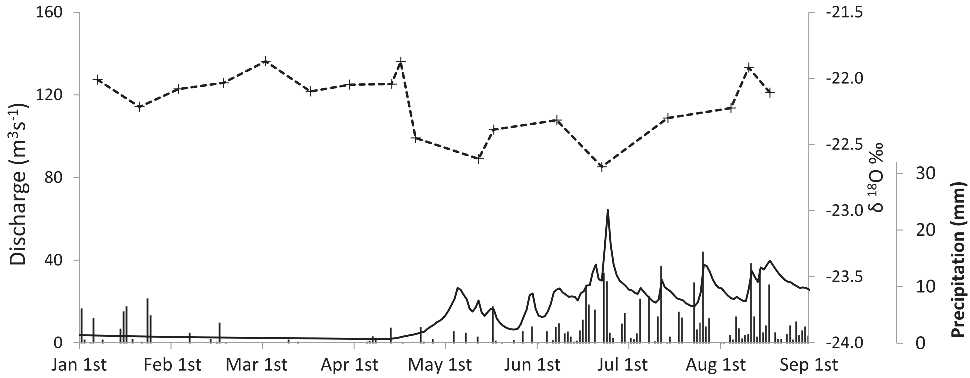

Figure 6. Oxygen-18 time series for the NKR for 2014. Dotted line: deuterium, thin full line: discharge.

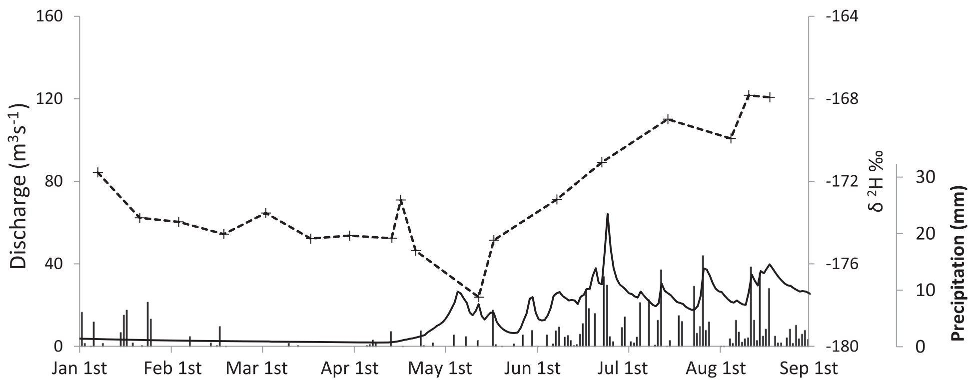

Figure 7. Deuterium time series for the NKR for 2014. Dotted line: deuterium, thin full line: discharge.

Eight water samples of the NKR were analysed for tritium concentrations for the year of 2014 (Figure 8). Baseflow during the winter months has the lowest tritium values but only marginally less than the 10 TU found for mean tritium in precipitation at Anchorage, Alaska, since 1990 [38], suggesting a subsurface mean residence time of less than about five years. The highest tritium concentrations were found at the beginning of May coincident with the onset of the spring freshet, with the lowest values observed a week later on 19 May. This rapid rise and decline suggests strong heterogeneity associated with winter and spring precipitation, and reflects the rapid hydraulic response of this watershed.

4.4. Seasonal evolution of major ion geochemistry of the NKR

NKR discharge is dominated by Ca–SO_4–HCO_3 geochemistry (Figure 9). Major ion data are consistent with carbonate and shale weathering following recharge through highly organic soils with high P_{CO2}. In contrast, K, released by degradation of biomass, varies inversely with these major ions and is a tracer for shallow drainage from soil. Calcite saturation throughout the year shows a system very close to saturation (baseflow: −0.51;

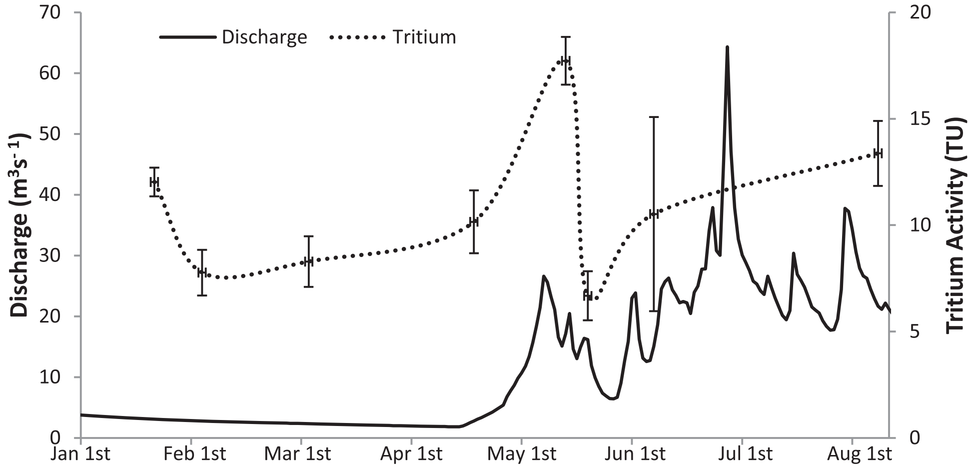

Figure 8. Measured tritium activity (expressed as TU) and total river discharge in the NKR, 2014.

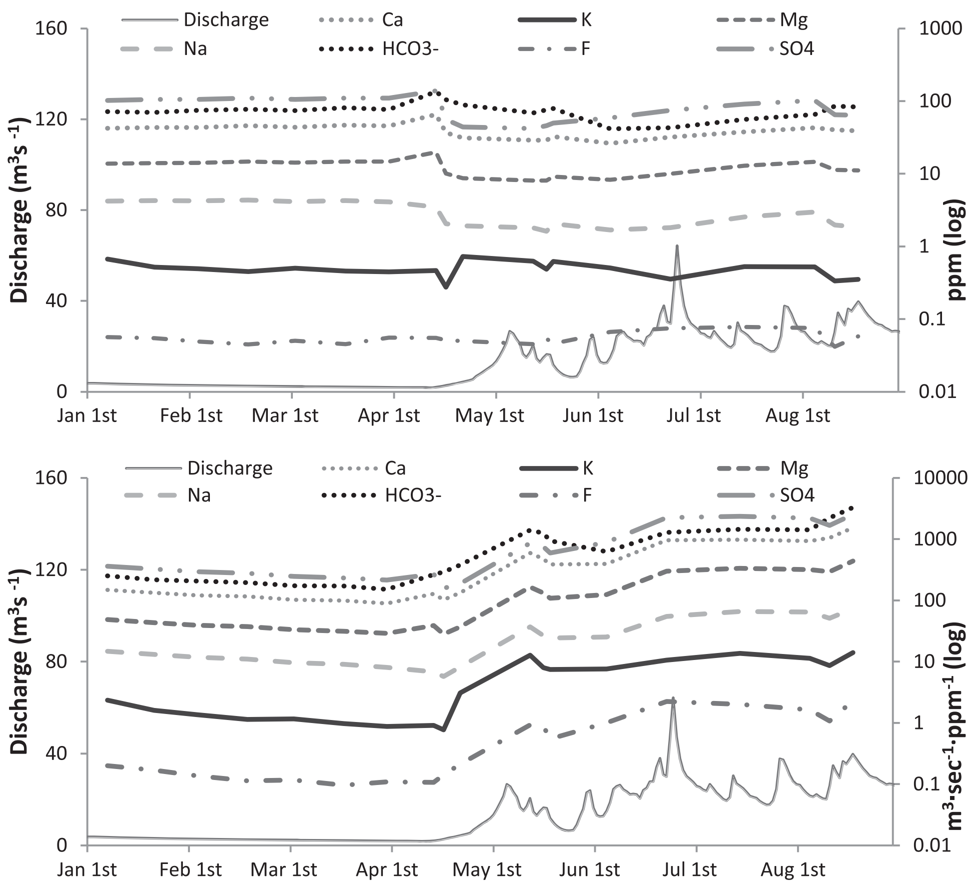

Figure 9. Time series of geogenic solutes in the NKR for 2014, expressed as both concentration (ppm) and flux ($m^3{\cdot}s^{-1}{\cdot}ppm^{-1}$).

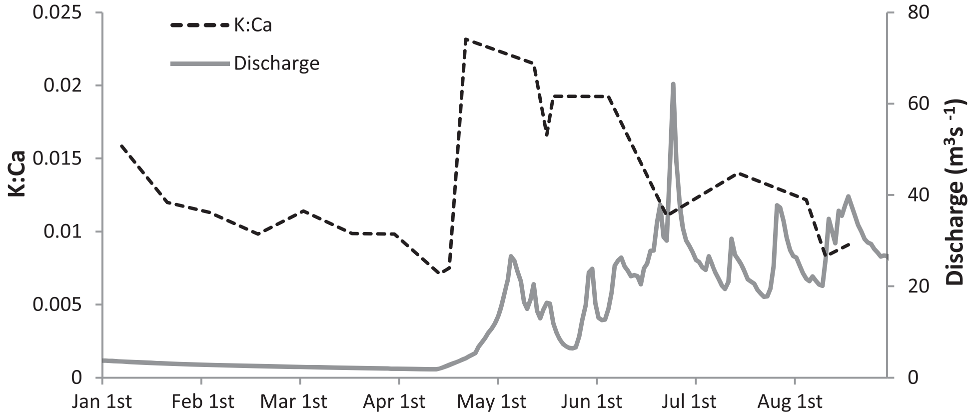

Figure 10. Time series of K:Ca concentrations in the NKR for 2014, showing the contribution of near surface water.

freshet: −0.82; summer: −0.37). Early, pre-freshet data are invariant, but the geogenic solutes (Ca^{2+}, Mg^{2+} and SO_4^{2-}) uniformly exhibit a 10–20 % spike in concentration at the immediate onset of increased flow, followed by a 20–40 % decrease 3 days later, which is attributed to the spring acid flux typically associated with the initial snowpack meltwater in nival watersheds. As snowmelt begins to contribute to discharge, solute concentrations begin to gradually dilute and achieve a local minimum during peak freshet. Despite the dilution, solute flux increases as discharge increases. Following the meltwater freshet by July, the concentrations begin to recover to pre-freshet levels, but show a greater variability in late spring and into summer. Ions and constituents that are more biologically active (K^+) show an inverse relationship with an increase from baseflow concentrations occurring during and following the spring freshet (Figure 10). No correlations were observed between discharge and dissolved solutes, as seen in other hydrological studies in discontinuous permafrost catchments [23,26].

4.5. Dissolved carbon of the NKR

The concentrations of DIC and DOC, together with their ^{13}C and ^{14}C contents show insightful trends in the sources of carbon during the transition from baseflow to spring freshet and over the summer melt season. DIC is steady near 15 ppm with an enriched $\delta^{13}C$ value of −8.8 ‰ during the winter months prior to river break (Figure 11) but spikes to the largest observed concentration of 25 ppm (135 ppm HCO_3^-), with slight enrichment in ^{13}C and decrease in ^{14}C at the very onset of increased flow when geogenic solutes spike. Although these enriched levels can be generated by exchange with carbonate bedrock in the flow system, a much lower ^{14}C activity (Table 1) would be anticipated. In fact, ^{14}C of DIC is quite close to that of DOC, and precludes extensive closed-system exchange with carbonate bedrock. Methanogenesis, however, can also generate enriched ^{13}C. This has been observed in permafrost catchments including the Firth River and Joe Creek in the northern Yukon [44]. DIC then decreases to less than 10 ppm with a steady increase in $\delta^{13}C$ to −6.3 ‰ during the period of snowmelt, then recovering to baseflow concentrations by the end of August. The trend for $\delta^{13}C$ of DIC shows inflections

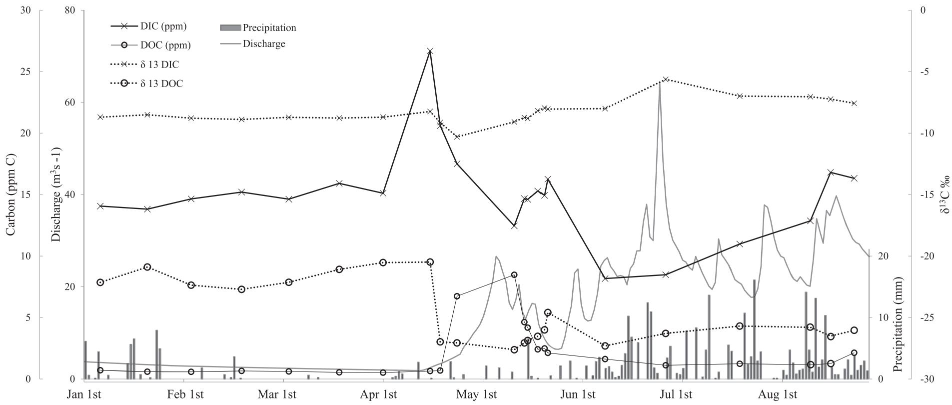

Figure 11. Dissolved carbon content in the NKR from 7 January to 19 August, 2014. Carbon concentrations are expressed as ppm of pure C; $\delta^{13}C$ is expressed relative to VPDB.

corresponding to changes in DIC concentration throughout the spring and summer, signifying different origins with varying degrees of mineral weathering vs. respired (organic) soil CO_2. The decrease in DIC at the onset of spring freshet is accompanied by a decrease in $\delta^{13}C_{DIC}$ due to inputs of soil CO_2. Radiocarbon activity is consistent, increasing from a baseflow value of 0.61 MC (fraction modern carbon) to 0.78 MC due to the input of oxidized soil organic carbon. DIC concentrations then recover from this spring freshet dilution with soil organics towards the baseflow groundwater values observed prior to spring freshet.

DOC trends support this seasonal variation in carbon outputs, showing a dramatic spike from <1 ppm prior to the freshet to 8.5 ppm C. This rise in DOC has been observed during spring freshet events in other rivers within discontinuous permafrost [2,16,17,25,26]. This correlates with an increase in K^+ and K^+/Ca^{2+}, and signifies a component derived from the soil zone. This DOC has more depleted ^{13}C (−27 ‰) and higher ^{14}C activity (0.94 MC) and

Table 1. Fraction modern carbon expressed as $^{14}C/^{12}C$ for dissolved carbon in the NKR from 7 January to 20 May.

	^{14}C DIC	±
7 January 2014	0.61	3.16×10^{-3}
21 January 2014	0.61	2.30×10^{-3}
3 February 2014	0.63	2.20×10^{-3}
18 February 2014	0.60	2.96×10^{-3}
4 March 2014	0.62	2.20×10^{-3}
19 March 2014	0.61	3.07×10^{-3}
1 April 2014	0.62	2.95×10^{-3}
15 April 2014	0.49	2.54×10^{-3}
18 April 2014	0.65	3.24×10^{-3}
23 April 2014	0.70	3.99×10^{-3}
10 May 2014	0.77	2.50×10^{-3}
13 May 2014	0.73	4.16×10^{-3}
14 May 2014	0.78	2.70×10^{-3}
19 May 2014	0.74	2.60×10^{-3}
20 May 2014	0.73	3.85×10^{-3}
	^{14}C DOC	±
18 February 2014	0.56	3.51×10^{-3}
23 April 2014	0.94	4.81×10^{-3}

represents a new source of carbon in the discharge derived from the soil zone during spring runoff. This influx of modern carbon during and after the river breaks is consistent with other studies [27,29,45]. Over the summer, dissolved carbon slowly recovers to base-flow values associated with old recalcitrant organic carbon discharging from the deep groundwater flow system.

4.6. Seasonal groundwater contribution to the NKR for 2014

A three-component hydrograph was used to model mixing of precipitation/runoff with the two dominant hydrological components including deep groundwater and soil/active layer groundwater. Sulphate was used as the geogenic solute, with both K^+ and DOC tested as pedogenic solutes. Results are shown in Figure 12, with consistent results for both pedogenic solutes. Discharge during the pre-freshet period was used to calibrate the deep

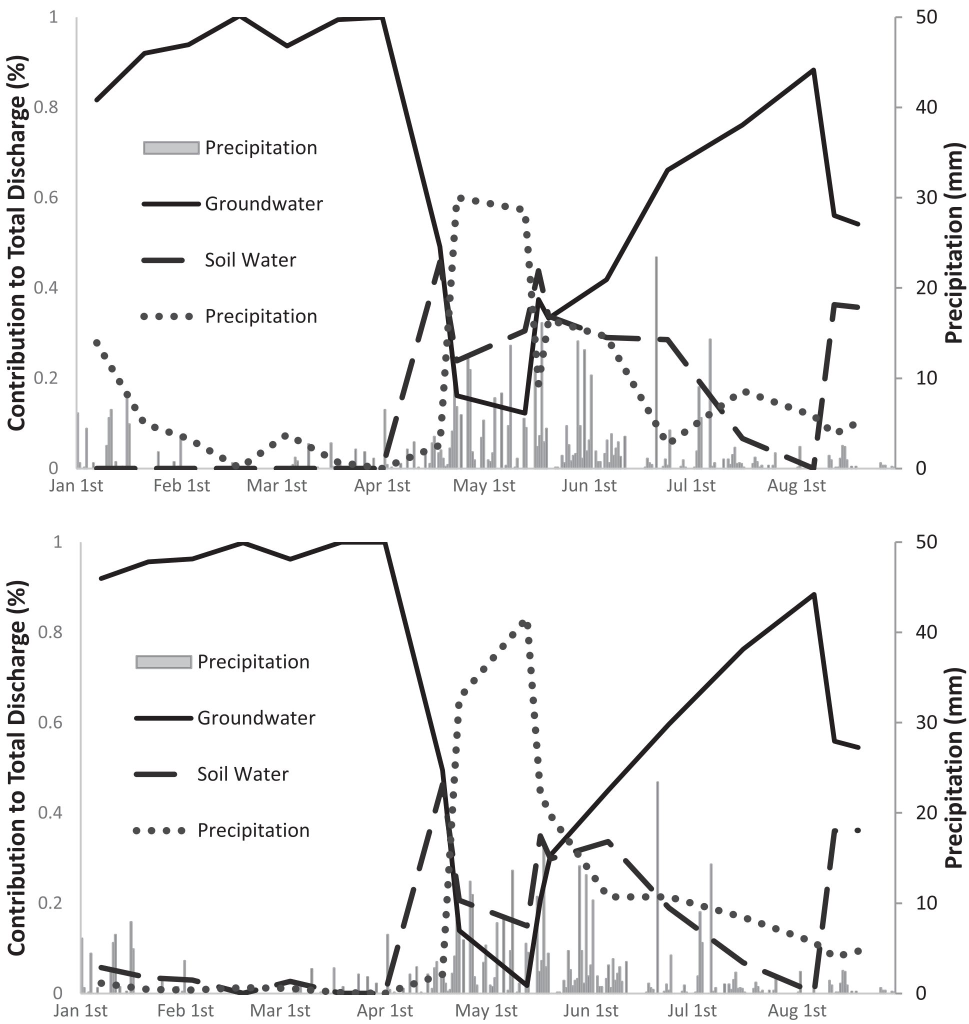

Figure 12. Three-component hydrograph separation using SO_4^{2-} as geogenic solute and K^+ (top chart) and DOC (bottom chart) as pedogenic solutes, expressed as percent of total discharge ($m^3{\cdot}s^{-1}{\cdot}ppm^{-1}$).

groundwater endmember which is represented at close to 100 % of the declining river discharge. Deep groundwater continues to decline through the early spring freshet, when discharge is comprised principally of direct runoff and soil water. However, by late spring (post snowmelt), when the active layer is expanding, the deep groundwater component increases to over 70 % of discharge by July. This growing contribution of deep groundwater over the melt season suggests that recharge through talik in the watershed is rapid. This further indicates that for most of the year, deep groundwater circulation dominates the hydrograph in this watershed. These results are consistent with other studies performed in sub-alpine catchments, albeit at lower latitudes [26], and even between studies of large headwater catchments [23].

5. Summary and conclusions

Historical records of discharge from the NKR show a significant correlation between total annual flow and baseflow. This relationship is intuitive as total annual discharge is a product of baseflow plus active layer flow. This positive trend in baseflow is consistent with other large river basins [2] in the Arctic and sub-Arctic, and suggests the NKR basin may be experiencing increased recharge of deep groundwater through expansion of talik related to climate warming. This underlines the need for simultaneous monitoring of both headwater catchments and sentinel tributaries. Wavelet analysis of historical discharge shows solar and climatic influences within this basin, with strength in spectral signals at 3–5 years from El Niño and 11-year solar cycles as well as a two to three decade PDO cycle.

Hydrograph separations were determined using sulphate as the dominant geogenic solute and potassium plus DOC as principal tracers for soil and active layer drainage. Results show a high runoff coefficient, with over 80 % of annual precipitation leaving the basin as river discharge. Nonetheless, hydrograph separation shows that discharge is dominated by deeply circulating groundwater, decreasing from near 100 % during late winter baseflow to less than 20 % during spring freshet and recovering to over 90 % by the end of the melt season. The balance is contributed by soil water drainage from the active layer and direct runoff of precipitation and snowmelt. The steady increase in the contribution of groundwater component to discharge following the spring freshet suggests a rapidly circulating groundwater system. Tritium data suggest subsurface residence times of less than five years. The decrease in this component to the low discharge levels observed by late winter suggests low storage in the basin, typical of fractured bedrock aquifers.

The narrow range for stable isotope values of the NKR ($\delta^{18}O = -22.3 \pm 0.3$ ‰) is depleted relative to spring and summer precipitation values (mean of -16.8 ± 4.2 ‰), and suggests that groundwater is significantly recharged by snowmelt. This is consistent with other findings for higher latitudes [36,46] and due to the comparatively shorter melt season and the more intense input from the spring freshet. Nonetheless, elevated carbon contents and high calculated P_{CO2} values suggest that groundwater recharge occurs by infiltration through soil where significant soil CO_2 and carbonate weathering takes place. Understanding specific recharge pathways in permafrost regions will be instrumental in understanding changes in large permafrost watersheds.

The dominance of groundwater as a component of the late melt season hydrograph, when the active layer thickness is maximized, emphasizes the importance of groundwater recharge and circulation even in permafrost catchments. This dominance of deep groundwater in the hydrograph may play a role in permafrost degradation under a regime of warming climate, through advection of enthalpy into the subsurface and contributing to the observed increase of baseflow discharge over the past five decades [2,22,24,47].

There is a considerable difference in sources of carbon exported by the NKR between winter baseflow, spring freshet and summer. Using both ^{13}C and radiocarbon, we were able to identify the recharge pathways and contributing fractions for different water components to a greater degree of certainty then with dissolved ions alone. The data collected from the NKR during 2014 support a model for a groundwater-dominated hydrological system with low storage that rapidly responds to meltwater recharge and precipitation. While groundwater discharge over the winter period represents only 21 % of annual discharge, this component increases during spring freshet and summer flow contributing almost 50 % of total river discharge.

Disclosure statement

No potential conflict of interest was reported by the authors.

References

[1] Serreze MC, Walsh JE, Chapin FS, et al. Observational evidence of recent change in the northern high-latitude environment. Clim Change. 2000;46:159–207.
[2] Walvoord MA, Striegl RG. Increased groundwater to stream discharge from permafrost thawing in the Yukon River basin: potential impacts on lateral export of carbon and nitrogen. Geophys Res Lett. 2007;34(12):L12402.
[3] Bring A, Fedorova I, Dibike Y, et al. Arctic terrestrial hydrology: a synthesis of processes, regional effects, and research challenges. J Geophys Res Biogeosci. 2016;121:621–649.
[4] Osterkamp TE. Characteristics of the recent warming of permafrost in Alaska. J Geophys Res Earth Surf. 2007;112(2):F02S02.
[5] Romanovsky VE, Smith SL, Christiansen HH. Permafrost thermal state in the polar Northern Hemisphere during the international polar year 2007–2009: a synthesis. Permafr Periglac Process. 2010;21(2):106–116.
[6] Yang ZP, Ou YH, Xu XL, et al. Effects of permafrost degradation on ecosystems. Acta Ecol Sin. 2010;30:33–39.
[7] Woo MK, Kane DL, Carey SK, et al. Progress in permafrost hydrology in the new millennium. Permafr Periglac Process. 2008;119(2):237–254.
[8] Carey SK, Pomeroy JW. Progress in Canadian snow and frozen ground hydrology, 2003–2007. Can Water Resour J. 2009;34:127–138.
[9] Muskett RR, Romanovsky VE. Groundwater storage changes in arctic permafrost watersheds from GRACE and in situ measurements. Environ Res Lett. 2009;4:045009.
[10] Walvoord MA, Kurylyk BL. Hydrologic impacts of thawing permafrost – a review. Vadose Zone J. 2016;15(6):vzj2016.01.0010.
[11] Shiklomanov AI, Lammers RB, Vörösmarty CJ. Widespread decline in hydrological monitoring threatens Pan-Arctic Research. Eos Trans AGU. 2002;83(2):13–17.
[12] Jacques J-MS, Sauchyn DJ. Increasing winter baseflow and mean annual streamflow from possible permafrost thawing in the Northwest Territories, Canada. Geophys Res Lett. 2009;36(1): L01401.

[13] Frey KE, Siegel DI, Smith LC. Geochemistry of west Siberian streams and their potential response to permafrost degradation. Water Resour Res. 2007;43(3):W03406.
[14] Smith LC, Pavelsky TM, MacDonald GM, et al. Rising minimum daily flows in northern Eurasian rivers: a growing influence of groundwater in the high-latitude hydrologic cycle. J Geophys Res Biogeosci. 2007;112(4):G04S47.
[15] Oberman NG. Contemporary permafrost degradation of the EEuropean North of RRussia. In: Kane D, Hinkel K, editors. Proceedings of the Ninth International Conference on Permafrost; 2008, June 29–July 3; Institute of Northern Engineering, Fairbanks, Alaska: University of Alaska Fairbanks; 2008. p. 1305–1310.
[16] Carey SK, Quinton WL. Evaluating runoff generation during summer using hydrometric, stable isotope and hydrochemical methods in a discontinuous permafrost alpine catchment. Hydrol Process. 2005;19(1):95–114.
[17] Petrone KC, Jones JB, Hinzman LD, et al. Seasonal export of carbon, nitrogen, and major solutes from Alaskan catchments with discontinuous permafrost. J Geophys Res Biogeosci. 2006;111(2): G02020.
[18] Frey KE, McClelland JW. Impacts of permafrost degradation on arctic river biogeochemistry. Hydrol Process. 2009;23:169–182.
[19] Brabets TP, Walvoord MA. Trends in streamflow in the Yukon River Basin from 1944 to 2005 and the influence of the Pacific Decadal Oscillation. J Hydrol. 2009;371:108–119.
[20] Prokoph A, Adamowski J, Adamowski K. Influence of the 11 year solar cycle on annual streamflow maxima in Southern Canada. J Hydrol. 2012;442:55–62.
[21] Nalley D, Adamowski J, Khalil B, et al. Inter-annual to inter-decadal streamflow variability in Quebec and Ontario in relation to dominant large-scale climate indices. J Hydrol. 2016;536:426–446.
[22] Carey SK, Boucher JL, Duarte CM. Inferring groundwater contributions and pathways to streamflow during snowmelt over multiple years in a discontinuous permafrost subarctic environment (Yukon,: Canada). Hydrogeol J. 2013;21(1):67–77.
[23] Carey SK, Tetzlaff D, Buttle J, et al. Use of color maps and wavelet coherence to discern seasonal and interannual climate influences on streamflow variability in northern catchments. Water Resour Res. 2013;49(10):6194–6207.
[24] O'Donnell J, Aiken GR, Walvoord M, et al. Dissolved organic matter composition of winter flow in the Yukon River basin: Implications of permafrost thaw and increased groundwater discharge. Glob Biogeochem Cycl. 2012;26(4):GB0E06.
[25] Carey SK, Quinton WL. Evaluating snowmelt runoff generation in a discontinuous permafrost catchment using stable isotope, hydrochemical and hydrometric data. Nord Hydrol. 2004;35 (4):309–324.
[26] Boucher JL, Carey SK. Exploring runoff processes using chemical, isotopic and hydrometric data in a discontinuous permafrost catchment. Hydrol Res. 2010;41(6):508–519.
[27] Raymond PA, McClelland JW, Holmes RM, et al. Flux and age of dissolved organic carbon exported to the Arctic Ocean: a carbon isotopic study of the five largest arctic rivers. Glob Biogeochem Cycl. 2007;21:GB4011.
[28] Spencer RGM, Aiken GR, Wickland KP, et al. Seasonal and spatial variability in dissolved organic matter quantity and composition from the Yukon River basin, Alaska. Glob Biogeochem Cycl. 2008;22:GB4002.
[29] Aiken G, Spencer R, Striegl R, et al. Influences of glacier melt and permafrost thaw on the age of dissolved organic carbon in the Yukon River basin. Glob Biogeochem Cycl. 2014;28:525–537.
[30] Maclean R, Oswood MW, Irons JG III, et al. The effect of permafrost on stream biogeochemistry: A case study of two streams in the Alaskan (USA) taiga. Biogeochemistry. 1999;47(3):239–267.
[31] Hu X, Pollard WH. The hydrologic analysis and modelling of river icing growth, North Fork Pass, Yukon Territory. Canada. Permafrost Periglacial. 1997;8:279–294.
[32] Kojima S. Ecosystem types of boreal forest in the North Klondike River valley, Yukon Territory, Canada, and their productivity potentials. Environ Monit Assess. 1996,39:265–281.
[33] Geological Survey of Canada. Surveys and mapping branch. Permafrost and ground ice conditions of northwestern Canada; 1987: Map 1619A. Scale 1:1,000,000.

[34] St-Jean G. Automated quantitative and isotopic (^{13}C) analysis of dissolved inorganic carbon and organic carbon in continuous-flow using a total organic carbon analyser. Rapid Commun Mass Spectrom. 2003;17:418–428.
[35] Hoeg S, Uhlenbrook S, Leibundgut C. Hydrograph separation in a mountainous catchment – combining hydrochemical and isotopic tracers. Hydrol Process. 2000;14:1199–1216.
[36] Clark I, Fritz P. Environmental isotopes in hydrogeology. New York: Lewis; 1997.
[37] Klaus J, McDonnell JJ. Hydrograph separation using stable isotopes: review and evaluation. J Hydrol. 2013;505:47–64.
[38] Clark ID. Groundwater geochemistry and isotopes. Boca Raton (FL): CRC Press; 2015.
[39] Woo MK. Permafrost hydrology. Heidelberg: Springer; 2012.
[40] Hammer Ø, Harper D, Ryan P. PAST: paleontological statistics software package for education and data analysis. Palaeontol Electron. 2001;4(1):art. 4.
[41] Team R Core. R: a language and environment for statistical computing. Vienna: R Foundation for Statistical Computing; 2016. http://www.r-project.org.
[42] Trapletti A, Horknik K. Tseries: Time series analysis and computational finance. R Package Version 0.15-35; 2016.
[43] Church M. Hydrology and permafrost with reference to northern North America. In: Permafrost Hydrology, Proceedings of the Workshop Seminar. Ottawa: Canadian National Committee, International Hydrological Decade; 1974. Vol. 7, p. 7–20.
[44] Clark ID, Lauriol B. Aufeis of the Firth River basin, northern Yukon, Canada: insights to permafrost hydrogeology and karst. Arct Alp Res. 1997;29:240–252.
[45] Neff JC, Finlay JC, Zimov SA, et al. Seasonal changes in the age and structure of dissolved organic carbon in Siberian rivers and streams. Geophys Res Lett. 2006;33(23):L23401.
[46] Dunne T, Leopold LB. Water in environmental planning. New York: Macmillan; 1978.
[47] Utting N, Lauriol B, Mochnacz N, et al. Noble gas and isotope geochemistry in western Canadian Arctic watersheds: tracing groundwater recharge in permafrost terrain. Hydrogeol J. 2013;21:79–91.